ICOS INFRASTRUCTURES FOR PM FLUX MEASUREMENT

L. Bignotti [1,2], A. Finco [1], R. Marzuoli [1], R. Urgnani [1], G. Gerosa [1]

[1] Università Cattolica del Sacro Cuore, Department of Mathematics and Physics, Brescia, Italy

[2]KU Leuven, Department of Earth and Environmental Sciences, Leuven, Belgium

* Correspondence to giacomo.gerosa@unicatt.it

INTRODUCTION AND AIM OF THE RESEARCH

PM is major concern for its dangerous effects on human health. **Vegetated areas have been identified as a possible sink for PM,** however, the characterization of the exchange dynamics between vegetation and the atmosphere is still incomplete.

To gave insight into the interactions between the atmospheric PM and vegetation **continuous measurements of size-resolved concentration and fluxes were run from February to May and from September to December 2019 on the 42 m high ICOS tower of Bosco Fontana (IT-BFt , Marmirolo, MN, Italy).**

The aims of the reaserch were:

1) investigate the **seasonal evolution** of size-segregated aerosol fluxes**;**
2) Verify whether the **forest is a sink** for aerosol particles;
3) Study the **influence of the forest habitus** (leaf-on/ leaf-off) on vertical fluxes and verify whether a **relationship between LAI and PM** fluxes exists .
4) investigate the influence of **climatic drivers** on aerosol fluxes.

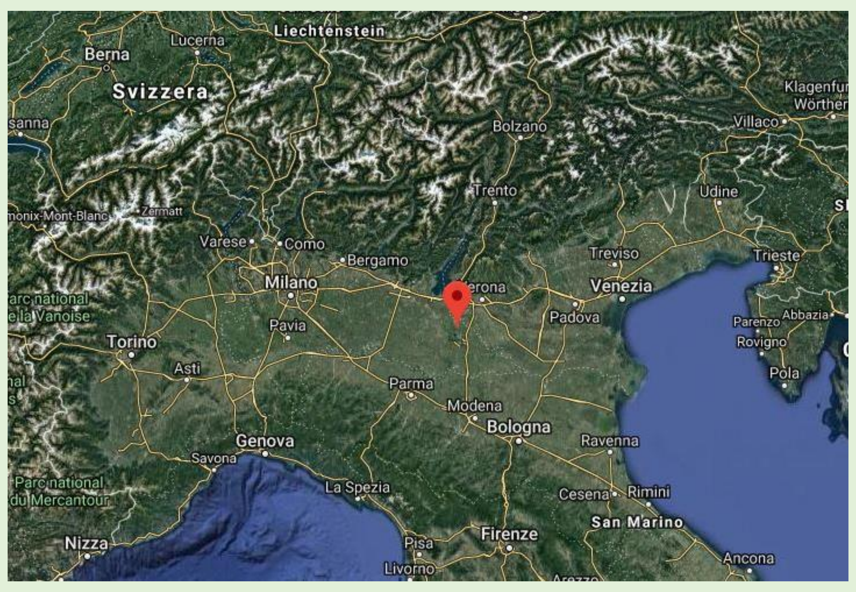

Figure 1 – Location of the measuring site in the natural reserve of Bosco Fontana (45°11'52.2" N, 10°44'31.2" E, 25 m a.s.l.), a oak-hornbeam ecosystem located at the outskirts of Mantua (Italy).

MATERIALS AND METHODS

Measurements of size-resolved PM concentration, wind components, sonic temperature and H_2O mixing ratio were performed at a height of 42 m with instruments sampling at a frequency of 10 Hz. See Fig.2 for instrument specifications.

Vertical fluxes of energy and matter were then calculated with the **eddy covariance technique**.

The flux of particles in a specific size-class *Fi* was obtained as the covariance between the vertical component of wind velocity *w* and the particle concentration in the selected size-class *Ci*.

$$F_i = \overline{w'C_i'}$$

While the exchange velocity v_e was determined as $v_e = -\frac{F_i}{C_i}$

ELPI+, Dekati, FI
Measures: Size-resolved aerosol concentration in 14 size-classes (from 0.006 µm to 10 µm)
Frequency 10 Hz

Metek, USA-1, DE
Mesaures: w, u, v, sonic temperature

Frequency 10 Hz (in this experiment)

Figure 2 – instrument details

RESULTS

Total PN daily fluxes **(Table 1)** revealed a different influence of the leaf habitus (leaf-on/leaf-off) on the fluxes of distinct aerosol size-classes.

Ultrafine particles (UFP) were emitted both in the leaf-on and the leaf-off period. Fine (FP) and coarse particles (CP) showed instead a reversal of their exchange direction between the two periods: fine particles, emitted in the leaf-off period, were deposited in presence of leaves, while coarse particles, emitted in the leaf-on period experimented a prevailing deposition in cooler leaf-off months, likely because of the heavier PM load.

Size-class (GMD)	F_N Leaf-on period (particles m^{-2} d^{-1})	Flux Direction	F_N Leaf-off period (particles m^{-2} d^{-1})	Flux Direction
1 (0.01 µm)	$2.39 \cdot 10^{11}$	↑	$2.48 \cdot 10^{11}$	↑
2 (0.02 µm)	$1.66 \cdot 10^{11}$	↑	$9.79 \cdot 10^{10}$	↑
3 (0.04 µm)	$8.31 \cdot 10^{10}$	↑	$5.91 \cdot 10^{10}$	↑
4 (0.07 µm)	$4.71 \cdot 10^{10}$	↑	$3.89 \cdot 10^{10}$	↑
5 (0.12 µm)	$2.69 \cdot 10^{8}$	↑	$2.51 \cdot 10^{10}$	↑
6 (0.20 µm)	$-3.44 \cdot 10^{10}$	↓	$1.56 \cdot 10^{10}$	↑
7 (0.31 µm)	$-4.59 \cdot 10^{10}$	↓	$5.82 \cdot 10^{9}$	↑
8 (0.48 µm)	$-2.36 \cdot 10^{10}$	↓	$7.92 \cdot 10^{7}$	↑
9 (0.76 µm)	$-1.81 \cdot 10^{9}$	↓	$1.59 \cdot 10^{8}$	↑
10 (1.24 µm)	$1.16 \cdot 10^{7}$	↑	$-1.94 \cdot 10^{7}$	↓
11 (2.01 µm)	$1.16 \cdot 10^{7}$	↑	$-1.94 \cdot 10^{7}$	↓
12 (3.01 µm)	$1.53 \cdot 10^{7}$	↑	$-2.62 \cdot 10^{6}$	↓
13 (4.43 µm)	$7.79 \cdot 10^{6}$	↑	$4.14 \cdot 10^{6}$	↑
14 (7.29 µm)	$-7.19 \cdot 10^{6}$	↓	$-1.63 \cdot 10^{7}$	↓

Table 1 - Daily number (F_N) fluxes obtained from the aerosol median daily cycles. Arrows indicate flux direction (upward=emission, downward=deposition).

The diel course of aerosol fluxes showed a **strong inter-month variability**. **UFP** (**Fig. 3**), which were prevalently deposited in the central part of the day in February, were **emitted from March onwards, increasing the intensity of their emission as leaves extended** and decreasing it with leaves senescence. In the same way, also **FP experimented a stronger deposition in late spring and early autumn months** (April and May and September).

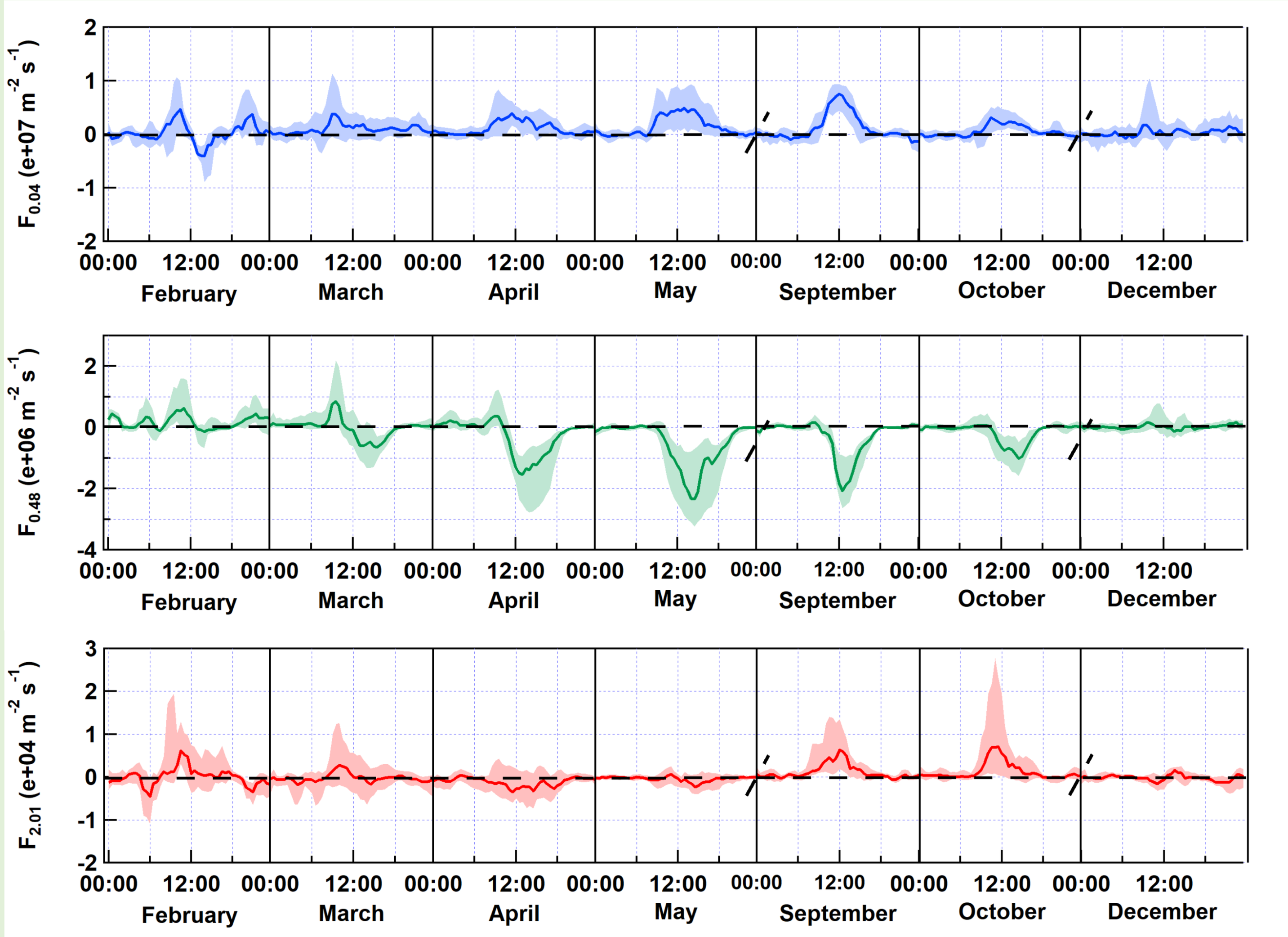

Figure 3 - Seasonal variation of three aerosol size-classes representing ultrafine, fine and coarse aerosol mode: a) class 3 (GMD=0.04 µm); b) class 7 (GMD=0.31 µm); c) class 11 (GMD=1.24 µm). Median fluxes are represented by continuous lines, while the dashed area is the IQR (inter-quartile range). The green and brown rectangles above the graphs provide indications about the leaf-on (green) and leaf-off months (brown).

The existence of a relationship between the intensity of the fluxes of UFP and FP and leaf development is confirmed by the scatter plots in **Fig. 4** that respectively report **a linear and exponential relationship between the LAI and the exchange velocity of UFP and FP**. For **CP non consistent patterns** were instead observed between the spring and the autumn leaf-on periods (**Fig. 3**) resulting in the absence of a relationship between their v_e and LAI.

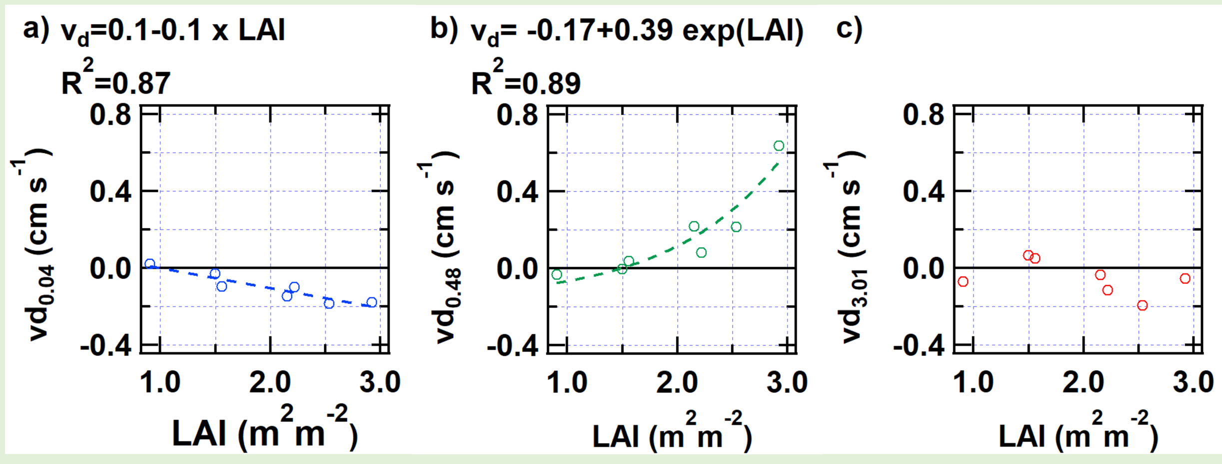

Figure 4 - scatter plots of monthly average of deposition velocities of a) Aitken; b) accumulation and c) coarse mode aerosols as a function of monthly LAI values.

The emission of **UFP was hypothesized to be related to stomatic processes** as the diel course of class 3 showed a striking similarity with that of the stomatal conductance to water g_{stom}, peaking almost at the same time and decreasing with the same pace (**Fig. 5**). On the contrary, class 8 (representing FP) peaked much later in the afternoon suggesting the deposition of FP is not a consequence of the stomatal uptake.

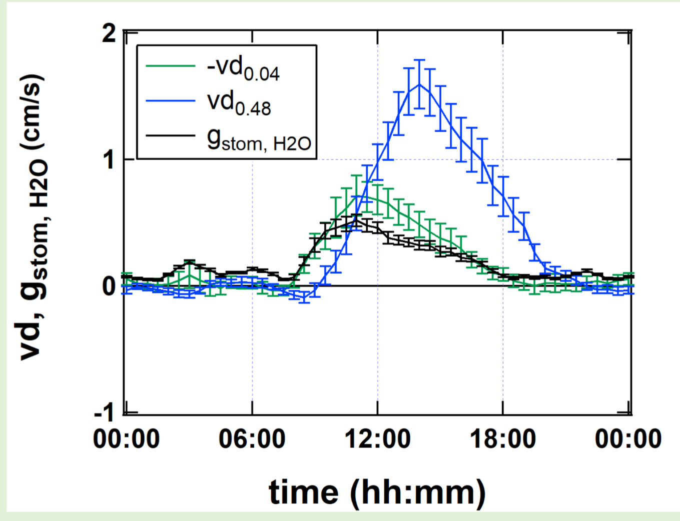

Figure 5 - Average diel behaviour of g_{stom} (black line) and deposition velocity of particles with GMD=0.04 µm (green line), and GMD=0.48 µm (blue line) for the month of May. Vertical bars represent the standard error of the mean. Please note that the sign of $v_{d,0.04}$ is reverted in order to better compare the diel course of particles with the one of g_{stom}

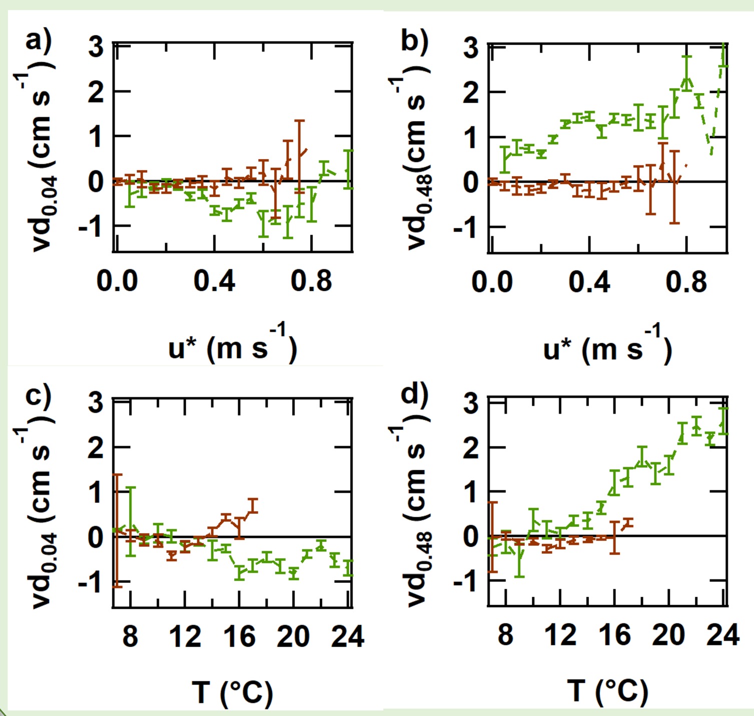

The meteorology of the site also played an active role on UFP and FP fluxes, especially in the leaf-on period. **The deposition velocities** of both modes showed indeed a **dependence from T and u*** (**Fig.6**), with u* enhancing both downward and upward vertical exchanges and T being hypothesized to drive gas-to-particle interconversion processes.

Figure 6 – dependence of ve from u* and T. Panels a) and c) refer to class 3 (GMD=0.04 µm, UFP) and b) and d) to class 8 (GMD=0.48 µm, FP). Brown and green colors represent the leaf-off and the leaf-on period, respectively.

CONCLUSIONS

Aerosol fluxes showed a seasonal variability

Empirical relations were found between LAI and the deposition velocity of UFP and FP

The presence of leaves affected aerosol vertical exchanges

u* and T emerged as drivers of aerosol fluxes

UFP emission at Bosco Fontana seemed related to stomatal activity